01 Jan 1971

A Gamma-Level Portable Ring-Core Magnetometer

Stanley V. Marshall
Missouri University of Science and Technology

Recommended Citation

S. V. Marshall, "A Gamma-Level Portable Ring-Core Magnetometer," *IEEE Transactions on Magnetics*, vol. 7, no. 1, pp. 183 - 185, Institute of Electrical and Electronics Engineers, Jan 1971.
The definitive version is available at https://doi.org/10.1109/TMAG.1971.1067000

A Gamma-Level Portable Ring-Core Magnetometer

STANLEY V. MARSHALL, MEMBER, IEEE

Abstract—A four-transistor circuit is described for a battery operated magnetometer that has 0.1 γ resolution using 1-in diameter 4–79 or 6–81 Mo–Permalloy tape cores of 20–40 Mx capacity. The center-tapped drive winding also serves as the sense winding, simplifying the sensor assembly. Some signal-to-noise results are presented to illustrate the fairly wide difference that may exist between cores of the same cross section and to demonstrate the advantage of reducing core area.

Introduction

A FEW years ago, the toroidal or ring-core sensor was considered relatively insensitive because of its large demagnetizing factor to the field being measured, and fluxgate sensors were usually constructed of one or two parallel strips of Mu metal or 4–79 Mo–Permalloy with various winding arrangements [1]. However, Geyger's work with ultrathin tape cores introduced the ring core as a competitor to other fluxgate sensors in sensitivity [2]. Closed core sensors require much less drive power, and the ring-core configuration lends itself to the construction of a two-axis sensor on the same core [3]. The demagnetizing factor for the ring-core sensor has essentially the same functional relation between core diameter and the square root of core cross section as that between length and diameter for a cylinder [4]. The demagnetizing factor for a 1-in diameter core whose cross section is made up of 12 wraps of 0.0005×0.062 in^2 tape is about the same as that of a cylindrical rod whose length-to-diameter ratio is 50. The Naval Ordnance Laboratory, Silver Spring, Md., recently developed a 6–81 Mo–Permalloy ring core with 0.1 γ peak-to-peak (0 to 10 Hz) noise level for the NASA Ames Research Center magnetometer using the mentioned dimensions [5].

Fig. 1. Portable magnetometer.

Manuscript received March 18, 1970; revised June 5, 1970, and September 10, 1970. Paper 10.6, presented at the 1970 INTERMAG Conference, Washington, D. C., April 21–24.

The author is with the Department of Electrical Engineering, the University of Missouri, Rolla, Mo. 65401.

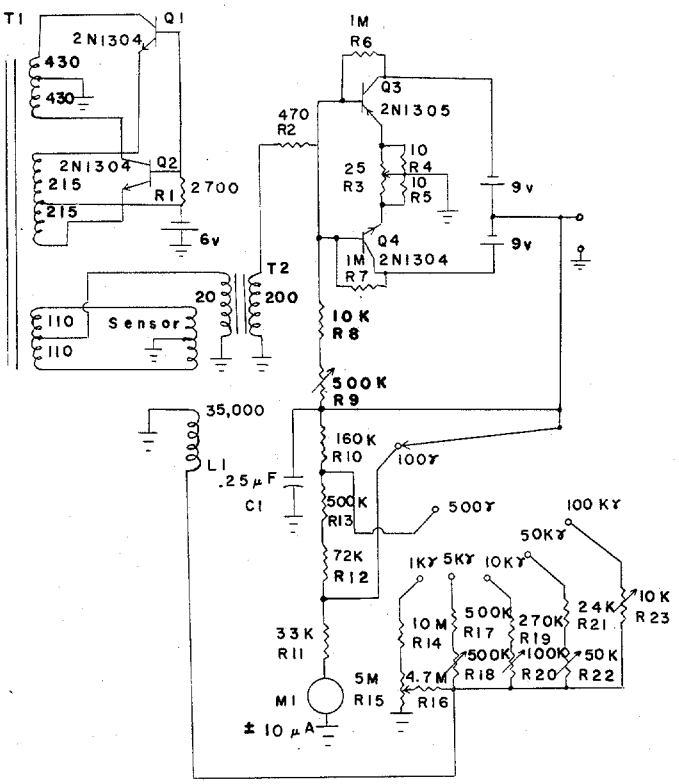

Fig. 2. Magnetometer circuit.

As a continuation of a recent paper, a compact fluxgate magnetometer circuit of gamma-level sensitivity which uses a toroidal sensor core is briefly described and results presented for the signal-to-noise performance for several different cores [6]. A model of the described instrument is shown in Fig. 1.

Circuit Description

A complete schematic of the magnetometer, except for the compensating field circuit, is shown in Fig. 2. Power for the circuit is supplied by four *D*-cells and two 9-V transistor batteries. Total power consumption varies from 30 to 100 mW depending on the size of base resistor R_1 for optimum performance.

The sensor output is the detector arm of a bridge consisting of the two halves of the sensor excitation winding and the center-tapped load winding of T_1. A sensor connected in this manner has been referred to as a "Brücken-

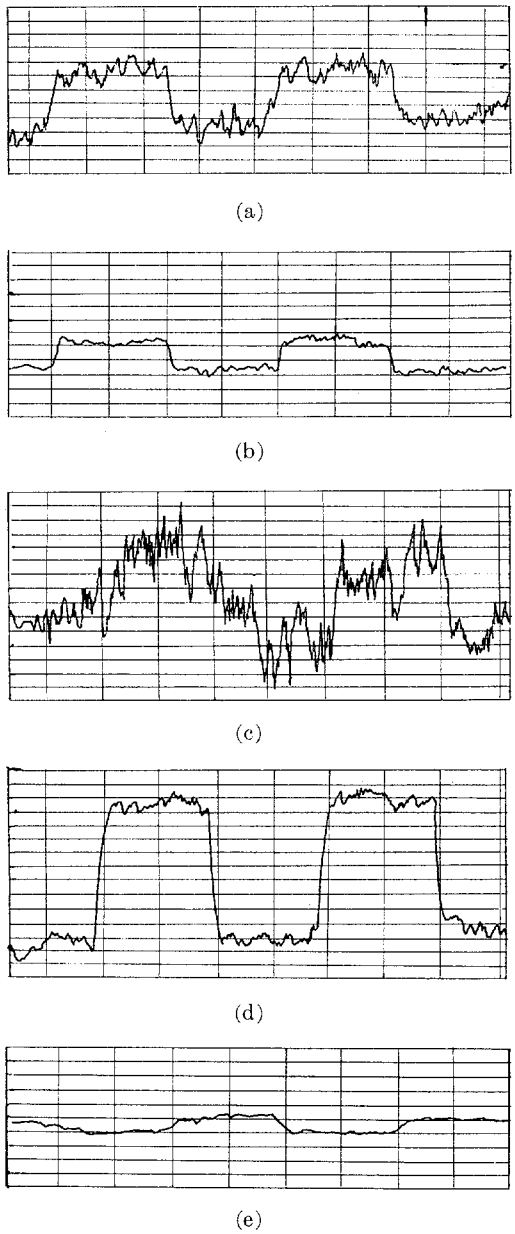

Fig. 3. Detector output for 0.25 Hz square wave applied field for various 1-in diameter sensors. (a) 40 wraps of $^1/_8$ in. $\times$ $^1/_8$ mil 4–79 Mo–Permalloy; drive winding = 400 turns, $\Delta H = 1\gamma$. (b) 20 wraps of $^1/_8$ in. $\times$ $^1/_4$ mil 4–79 Mo–Permalloy; drive winding = 400 turns, $\Delta H = 1\gamma$. (c) 10 wraps of $^1/_8$ in. $\times$ $^1/_2$ mil 4–79 Mo–Permalloy; drive winding = 400 turns, $\Delta H = 1\gamma$. (d) 9 wraps of $^1/_{16}$ in. $\times$ $^1/_2$ mil 6–81 Mo–Permalloy; drive winding = 400 turns, $\Delta H = 1\gamma$. (e) Approximately 50 wraps of $^1/_8$ in. $\times$ 1 mil 4–79 Mo–Permalloy; drive winding = 52 turns, $\Delta H = 10\gamma$, vertical scale = 1 mV/div; horizontal scale = 1 s/div.

sonden" [1]. Differential peak detection is accomplished by complementary transistors Q_3 and Q_4 which conduct on alternate half-cycles of the excitation period. The range of linearity of the detector depends on these transistors and the particular sensor core, and is limited to an output magnitude somewhat less than either 9-V supply battery.

Perhaps one of the most important features of the magnetometer described in this paper is the simplicity of the circuit and, in particular, the sensor construction. Starting with the commercially available ring core, a single center-tapped winding serves both as the drive and sense winding. In most designs the sense winding is a separate winding of at least several hundred turns.

Sensors

The magnetometer circuit was optimized for a 1-in diameter sensor core of 4–79 Mo–Permalloy of 40 Mx flux capacity. Initial tests were based on three cores of this size having 40 wraps of 1/8-mil tape, 20 wraps of 1/4-mil tape, and 10 wraps of 1/2-mil tape. The tape width was 0.125 in.

The sensor was placed in a flux tank for calibration and signal-to-noise measurements. The residual axial field in the flux tank was cancelled electrically in the detector by the balance adjustment. Since the basic detector is linear over a range of 1000 γ, and the residual field is on the order of 10 to 50 γ, electrical compensation for the residual field did not appreciably alter the symmetry of the detector output with respect to the input field.

In Fig. 3, the output of the detector is recorded for a number of different sensors, including a 6–81 Mo–Permalloy. The detector output was connected to the recorder through an RC network whose time constant was 0.15 s. The circuit has 0.1 γ resolution capability using the cores Fig. 3(b) and (d). Maximum output is obtained from the recording of Fig. 3(d) at approximately 10 mV/γ, and it should be noted that the demagnetizing factor for this core is about half that of the first three because of the narrower tape. The maximum resolution for the core of Fig. 3(e) is about 5 γ and the detector output is only about 1/100 of the output of Fig. 3(d) for the same input field, while its cross section is 20 times as great, and the demagnetizing factor is consequently much greater. However, the materials of even the first three cores of Fig. 3 are not exactly the same, and the distribution of the drive winding turns varied slightly between cores. It has been demonstrated by the author that the symmetry of the two halves of the drive winding with respect to the core tape ends can be a factor in the output noise, the null offset, and the sensitivity in mV/γ. In this instrument, null offset is a function of how well the complementary detector transistors are matched as well as any offset that is inherent to the sensor core. The detector balance is used to compensate for all sources of null offset, and the sources of offset are not important.

Conclusion

The magnetometer circuit described in this paper can provide for many applications when gamma-level resolutions are required and where low battery drain and a simple circuit construction are important. A comparison of a few cores of basically the same material (although of different processing) but of different core areas demonstrates the improvement in signal-to-noise when core area is reduced. However, there are obviously other important factors that influence the signal-to-noise capacility, since the three 40 Mx cores are quite different in this respect. These other

factors, although very important to measurements of 0.1 γ fields, are not necessarily important to applications where a noise level of a few gammas can be tolerated.

References

[1] J. Greiner, "Feldmessunger nach dem oberwellen, verfahren Sieb, und Differenzsnden," *Nachrtech.*, vol. 10, Apr. 1960, pp. 156–162.

[2] W. A. Geyger, "The ring-core magnetometer—a new type of second-harmonic flux-gate magnetometer," *AIEE Trans. Commun. Electron.*, vol. 81, Mar. 1962, pp. 65–73.

[3] M. H. Acuna and C. J. Pellerin, "A miniature two-axis fluxgate magnetometer," *IEEE Trans. on Geosci. Electron.*, vol. GE-7, Oct. 1969, pp. 252–260.

[4] S. V. Marshall, "An analytic model for the fluxgate magnetometer," *IEEE Trans. Mag.*, vol. MAG-3, Sept. 1967, pp. 459–463.

[5] D. I. Gordon, R. H. Lundsten, R. A. Chiarodo, and H. H. Helms, Jr., "A fluxgate sensor of high stability for low field magnetometry," *IEEE Trans. Magn.*, vol. MAG-4, Sept. 1968, pp. 397–401.

[6] S. V. Marshall, "Design and application for a portable gamma-level magnetometer," in *Proc. Nat. Electron. Conf.*, 1969, pp. 236–241.

Computation and Modeling of Eddy Currents in Tape-Wound Square-Loop Cores

DAVID NITZAN, SENIOR MEMBER, IEEE

Abstract—**Eddy currents in tape-wound cores are classified into microscopic and macroscopic eddy currents. The latter, denoted by i_e, exists during mode II among three switching modes. Inherent peak $\dot{\phi}$ versus F for a high $F = F_D$ drive is computed from measured $\dot{\phi}_m(F_D)$ and $\phi_m(F_D)$, the $\dot{\phi}$ and ϕ when $\dot{\phi}$ is maximum. The expected line density of reversed-domain nucleation centers is computed from $\phi_m(F_D)$. A switching tape-wound core is equivalent to one with "ferrite-core" characteristics that is loaded by a resistance $R_e = \dot{\phi}/i_e$. A special computer program was developed to compute $i_e(\phi,F_D)$ and $R_e(\phi,F_D)$; the higher F_D, the wider and lower the resulting U shaped $R_e(\phi)$. Domain-pattern models are proposed. Accordingly, $n_p(\phi,F_D)$ domains in which $\dot{\phi} \cdot p(\phi,F_D)$ is generated are encircled by macroscopic eddy currents where $n_p \geq 0$ and $1 \geq p \geq 0$. The semiempirical model $R_e(\phi,F_D) = R_{ez}(F_D)/\{1 - [\phi/\phi_m(F_D)]\}$, where R_{ez} is R_e at $\phi = 0$, is proposed. The functions describing $\phi_m(F_D)$ and $R_{ez}(F_D)$ include a total of five parameters besides ϕ_s.**

I. Introduction

THE LOSS mechanism in common ferrite cores involves spin-relaxation damping, which depends on the velocities of domain walls but not on their positions. Flux switching in tape-wound cores involves additional losses due to eddy currents [1]–[11]. Following Friedlaender [6], we shall distinguish between microscopic and macroscopic eddy currents. Microscopic eddy currents are local and depend only on the velocities of the domain walls. Their effect on the flux-switching process is thus indistinguishable from that of spin relaxation. Macroscopic eddy currents, on the other hand, encircle each domain whose flux changes; they depend on both the velocities and the positions of the domain walls.

Consider a tape-wound core that is switched by a step-MMF drive of amplitude $F_D = N_D I_D$. The effects of the macroscopic eddy currents on the resulting time rate of change of flux $\dot{\phi}(t)$ have been investigated in the past [1]–[11]. Depending on the strength of the applied magnetic field $H_{ap}(t)$, different models have been postulated for the shapes of the resulting moving domain walls. For a low H_{ap}, single and/or double planar walls parallel to the tape edges have been assumed [1], [2], [4]–[7]. For a high $H_{ap}(t)$, Williams *et al.* [1] assumed that flux switching in a silicon–iron crystal occurs by a collapsing cylindrical wall. Based on this assumption, they calculated $\dot{\phi}(t)$ for an infinitely long cylindrical core of a circular cross section.

Rodbell and Bean [5] proposed a physical model for high H_{ap} flux switching in square-loop metallic tapes. Their model is illustrated in Fig. 1, where w is the tape width and s is the tape thickness. Initially [Fig. 1(a)], nucleation-center sites of domains of reversed magnetization (pointing out of the paper in this example) are distributed randomly throughout the cross section of the tape (where the bulk magnetization points into the paper, as marked by x). Following the application of a step $H_{ap}(t)$, the reversed domains grow, as shown in Fig. 1(b), until they collide and their walls merge into the major domain walls shown in Fig. 1(c), at which time $\dot{B}(t)$ reaches a maximum value. Beyond this point, macroscopic eddy currents are generated in the region between the major domain walls and the tape surfaces [Fig. 1(d)] and partially shield the tape interior from the applied field. Consequently, the inward motion of the major walls slows down, interior reversed domains are blocked from further expansion (or even shrink), and $\dot{B}(t)$ decreases.

Manuscript received May 12, 1970; revised July 10, 1970. Paper 30.1, presented at the 1970 INTERMAG Conference, Washington, D. C., April 21–24. This work was supported in part by the Harry Diamond Laboratories, Washington, D. C., under contract DAAG 39-68-C-0071, and in part by the Defense Atomic Support Agency under NWER Subtask TC011.

The author is with the Stanford Research Institute, Menlo Park, Calif.